J. Mater. Environ. Sci. 5 (1) (2014) 81-94
ISSN : 2028-2508
CODEN: JMESCN

Experimental and theoretical investigations anti-corrosive properties of Menthone on mild steel corrosion in hydrochloric acid

A. Ansari[1], M. Znini[1], I. Hamdani[3], L. Majidi[2*], A. Bouyanzer[3], B. Hammouti[3,4]
[1]*Université My Ismail, Faculté Polydisciplinaire, BP 512, 52003, Errachidia, Morocco*
[2]*Université My Ismail, Laboratoire des Substances Naturelles & Synthèse et Dynamique Moléculaire, Faculté des Sciences et Techniques, BP 509, 52003, Errachidia, Morocco.*
[3]*Laboratoire de Chimie Appliquée et Environnement, Faculté des Sciences, Oujda, Morocco.*
[4] *Petrochemical Research Chair, Chemistry Department, College of Science, King Saud University, P.O. Box 2455, Riyadh 11451, Saudi Arabia.*

Received 27 Aug 2013, Revised 24 Sept 2013, Accepted 24 Sept 2013
** Corresponding Author: e- mail : lmajidi@yahoo.fr Tel: (+212) 05 35 57 0024; Fax : (+212) 05 35 57 43 07*

Abstract
The inhibition of menthone (MAN) on the corrosion of mild steel in 1 M HCl was studied by gravimetric as well as potentiodynamic polarization and electrochemical impedance spectroscopy (EIS) techniques at 298–333 K. Results obtained show that MAN act as inhibitor for mild steel in HCl solution. The inhibition efficiency was found to increase with increase in MAN concentration but decreased with temperature. Polarization measurements showed that the studied inhibitor is mixed type. EIS measurements revealed that the charge transfer resistance increases with increase in the concentration of inhibitor. The adsorption of the inhibitor on the mild steel in the acid solution was found to accord with Langmuir's adsorption isotherm at all the concentrations and temperatures studied. Phenomenon of physical adsorption is proposed from the activation parameter obtained. Thermodynamic parameters reveal that the adsorption process is spontaneous. Quantum chemical calculations using DFT were used to calculate some electronic properties of the molecule in order to ascertain any correlation between the inhibitive effect and molecular structure of menthone.

Keywords: Menthone**;** Mild steel; Corrosion inhibitor; Density functional theory (DFT); HCl

Introduction
The corrosion of steel is the most common form of corrosion, especially in acid solution. Hydrochloric acid is also an important mineral acid with many uses in the same systems and leads the researchers to the study of the effect of the corrosion inhibitors [1–3]. Most corrosion inhibitors are synthetic organic compounds having hetero atoms in their aromatic or long carbon chain [4]. These organic compounds can adsorb on the metal surface, block the active sites on the surface and thereby reduce the corrosion rate. However, the toxic effects of most synthetic corrosion inhibitors, the obligations of health and human security have led to the research of green alternatives that are environmentally friendly and harmless [4-6]. Thus, the researches have been focused on the use of eco-friendly compounds and ecologically acceptable such as extract of common plants because to bio-degrability, eco-friendliness, low cost and easy availability and renewable sources of materials [7, 8]. Recently, several our studies have been carried out on the inhibition of corrosion of steel by natural products such as essential oils and its major components [9-12]. In continuation of our work on development of green corrosion inhibitors, the present study investigates the inhibiting effect of menthone against corrosion of mild steel in HCl media. Menthone (Figure 1), a cyclic monterpenoid, is naturally occurring component of some volatile essential oils, most notably those from various *Mentha* species, especially pennyroyal and peppermint. This terpenoid substance is a colorless or pale yellow liquid, with a mint-like odor similar to that of menthol and is used in food industry as a flavoring ingredient, in perfumes compositions and other fragrance products [13]. The objective of the present work is to study the inhibitive action of menthone (MAN) as a green and naturally occurring substance on corrosion behavior of mild steel in 1M HCl solution using weight loss, potentiodynamic polarization curves and electrochemical impedance spectroscopy (EIS) methods. The thermodynamic parameters describing the kinetic of corrosion as well as the adsorption process when varying temperature and concentration of menthone are evaluated and discussed.

ISSN : 2028-2508
CODEN: JMESCN

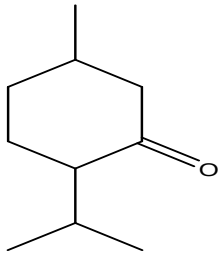

Figure. 1. Molecular structure of menthone (MAN).

Materials and methods

1. Preparation of materials

Mild steel coupons containing 0.09 wt.% (P), 0.38 wt.% (Si), 0.01 wt.% (Al), 0.05 wt.% (Mn), 0.21 wt.% (C), 0.05 wt.% (S) and the remainder iron (Fe) used for weight loss measurements. The surface preparation of the mild steel coupons (2 cm x 2 cm x 0.05 cm) was carried out with emery papers by increasing grades (400, 600 and 1200 grit size), then degreased with AR grade ethanol and dried at room temperature before use. The aggressive solutions of 1 M HCl was prepared by dilution of analytical grade 37% HCl with double distilled water. Menthone was isolated by fractionation of essential oil of *Mentha rotundifilia* (69.1 % pulegone and 18.5 % menthone) and its concentration range was 0.81-6.48 mM (0.125-1 g/L). All reagents used for the study were of analytical grade.

2. Electrochemical studies

Electrochemical measurements were carried out in a conventional three-electrode electrolysis cylindrical Pyrex glass cell. The working electrode (WE) in the form of disc cut from steel has a geometric area of 1 cm^2 and is embedded in polytetrafluoroethylene (PTFE). A saturated calomel electrode (SCE) and a disc platinum electrode were used respectively as reference and auxiliary electrodes, respectively. The temperature was thermostatically controlled at 303 K. The WE was abraded with silicon carbide paper (grade P1200), degreased with AR grade ethanol and acetone, and rinsed with double-distilled water before use.

3. Potentiodynamic polarization curves

Polarization curves studies were carried out using EG&G Instruments potentiostat-galvanostat (Model 263A) at 303 K without and with addition of various concentrations of inhibitor in 1 M HCl solution at a scan rate of 0.5 mV/sec. Before recording the cathodic polarisation curves, the mild steel electrode is polarised at -800 mV for 10 min. For anodic curves, the potential of the electrode is swept from its corrosion potential after 30 min at free corrosion potential, to more positive values. The test solution is deaerated with pure nitrogen. Gas bubbling is maintained through the experiments. In the case of polarization method the relation determines the inhibition efficiency (E_I %):

$$E_I\,\% = \frac{I_{corr} - I_{corr\ (inh)}}{I_{corr}} \times 100 \qquad (1)$$

where I_{corr} and $I_{corr\ (inh)}$ are the corrosion current density values without and with the inhibitor, respectively, obtained by extrapolation of cathodic and anodic Tafel lines to the corrosion potential.

4. Electrochemical impedance spectroscopy (EIS)

The electrochemical impedance spectroscopy (EIS) measurements were carried out with the electrochemical system which included a digital potentiostat model Volta lab PGZ 100 computer at E_{corr} after immersion in solution without bubbling, the circular surface of mild steel exposing of 1 cm^2 to the solution were used as working electrode. After the determination of steady-state current at a given potential, sine wave voltage (10 mV) peak to peak, at frequencies between 100 kHz and 10 mHz were superimposed on the rest potential. Computer programs automatically controlled the measurements performed at rest potentials after 30 min of exposure.

The impedance diagrams are given in the Nyquist representation. Values of R_t and C_{dl} were obtained from Nyquist plots. The charge-transfer resistance (R_t) values are calculated from the difference in impedance at lower and higher frequencies, as suggested by Tsuru et *al*. [14] The inhibition efficiency got from the charge-transfer resistance is calculated by the following relation:

$$E_{Rt}\,\% = \frac{R'_t - R_t}{R'_t} \times 100 \qquad (2)$$

where R_t and R'_t are the charge-transfer resistance values without and with inhibitor respectively. R_t is the diameter of the loop.

The double layer capacitance (C_{dl}) and the frequency at which the imaginary component of the impedance is maximal ($-Z_{max}$) are found determined by Eq. (3):

$$C_{dl} = \frac{1}{\omega . R_t} \quad \text{where} \quad \omega = 2\,\pi\,.\,f_{max} \qquad (3)$$

Impedance diagrams are obtained for frequency range 100 KHz –10 mHz at the open circuit potential for mild steel in 1 M HCl in the presence and absence of inhibitor.

5. Weight loss measurements

Weight loss tests were carried out in a double walled glass cell equipped with a thermostat-cooling condenser. The solution volume was 100 mL with and without the presence of different concentrations of MAN ranging from 0.81 to 6.48 mM at various temperatures (303-343 K). After 6 h of immersion, the specimens of steel were carefully washed in double-distilled water, dried and then weighed. The rinse removed loose segments of the film of the corroded samples. Triplicate experiments were performed in each case and the mean value of the weight loss is reported using an analytical balance (precision ± 0.1 mg). Weight loss allowed us to calculate the mean corrosion rate as expressed in $mg.cm^{-2}\ h^{-1}$. The corrosion rate (W_{corr}) and inhibition efficiency E_w (%) were calculated according to the Eqs. (4) and (5) respectively:

$$W = \frac{\Delta m}{St} \qquad (4)$$

$$E_W\ \% = \frac{W_{corr} - W_{corr\ (inh)}}{W_{corr}} \times 100 \qquad (5)$$

where Δm (mg) is the specimen weight before and after immersion in the tested solution, W_{corr} and $W_{corr(inh)}$ are the values of corrosion weight losses ($mg/cm^2.h$) of mild steel in uninhibited and inhibited solutions, respectively, S is the area of the mild steel specimen (cm^2) and t is the exposure time (h). The degree of surface coverage was calculated using:

$$\theta = \frac{W_{corr} - W_{corr\ (inh)}}{W_{corr}} \qquad (6)$$

where θ is surface coverage; $W_{corr(inh)}$ is corrosion rate for steel in presence of inhibitor, W_{corr} is corrosion rate for steel in the absence of inhibitor.

6. Computational details

In the last few decades, theoretical investigations based on quantum chemical calculations have been proposed as a powerful tool for predicting a number of molecular parameters directly related to the corrosion inhibiting property of any chemical compound [15]. Among several theoretical methods available, the density functional theory (DFT) is one of the most important theoretical models used to analyze the characteristics of the inhibitor/surface mechanism and to describe the structural nature of the inhibitor on the corrosion process [16]. B3LYP, a version of the DFT method that uses Becke's three parameter functional (B3) and includes a mixture of HF with DFT exchange terms associated with the gradient-corrected correlation functional of Lee, Yang and Parr (LYP) was used in this paper to carry out quantum calculations. Then, full geometry optimization together with the vibrational analysis of the optimized structures of the inhibitor was carried out at the (B3LYP/6-31G (d) level of theory. The following theoretical parameters for MAN molecule in neutral form by means of standard Gaussian 03 software package such as the energy of the highest occupied molecular orbital (E_{HOMO}), the energy of the lowest unoccupied molecular orbital (E_{LUMO}), $\Delta E_{gap} = E_{HOMO} - E_{LUMO}$, the dipole moment (μ) and total energy (TE) were calculated.

Results and discussion

1. Potentiodynamic polarization curves

Potentiodynamic anodic and cathodic polarization plots for mild steel specimens in 1 M HCl solution in the absence and presence of different concentrations of MAN at 308 K are shown in Figure 2. The respective kinetic parameters including corrosion current density (I_{corr}), corrosion potential (E_{corr}), cathodic slopes (β_c) and inhibition efficiency (IE%) are given in Table 1.

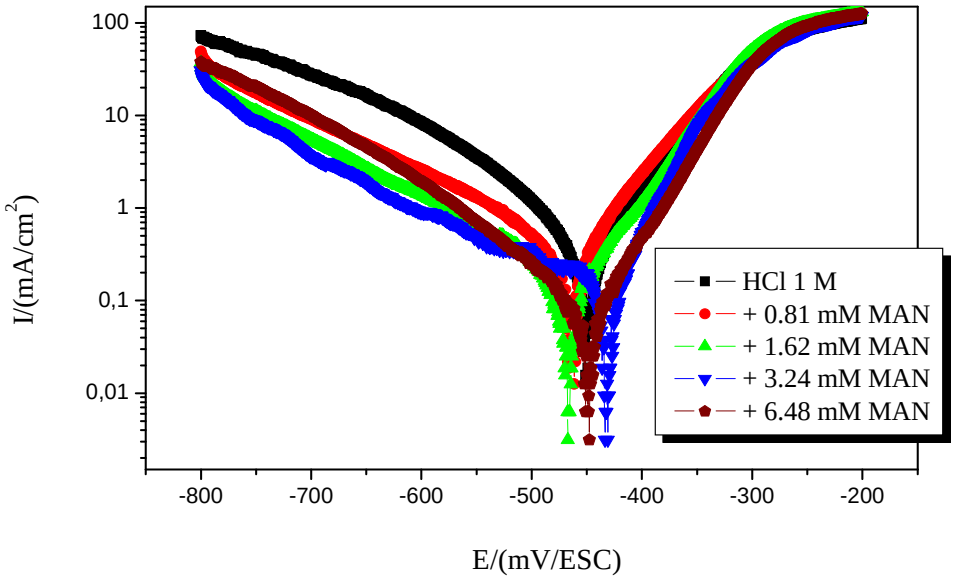

Figure 2. Anodic and cathodic polarization curves of mild steel in solutions of 1 M HCl in the presence and absence of different concentrations of MAN. **/SCE**

Inspection of Fig. 2 shows that the addition of MAN has an inhibitive effect in the both anodic and cathodic parts of the polarization curves. This indicates a modification of the mechanism of cathodic hydrogen evolution as well as anodic dissolution of steel, which suggest that inhibitor powerfully inhibits the corrosion process of mild steel, and its ability as corrosion inhibitor is enhanced as its concentration is increased. Further, the values of the cathodic Tafel slopes β_c, in the presence of the inhibitor, significantly change with the inhibitor concentration, which indicates the influence on the cathodic reactions and modifies the mechanism of hydrogen evolution reaction.

Table 1: Electrochemical parameters of steel at different concentrations of MAN studied in 1 M HCl at 308 K. Efficiencies corresponding corrosion inhibition.

concentration (mM)	E_{corr} (mV)	I_{corr} ($\mu A/cm^2$)	β_c (mV/dec)	IE %
HCl 1 M	-450	420	-105.2	
0.81	-464	281.1	-152.3	33
1.62	-467	167.8	-152.5	60
3.24	-432	70.7	-142.1	83
6.48	-449	42.3	-97.2	89

The analysis of the data in Table 1 revealed that the corrosion current densities (I_{corr}) decreases considerably with increasing the inhibitor concentration. Correspondingly, the inhibition efficiency (IE %), increases with the inhibitor concentration to reach its maximum value, 89 %, at 6.48 mM. This behaviour suggests that the MAN adsorption protective film formed on the carbon steel surface tends to be more and more complete and stable. The presence of inhibitor caused a slight shift of corrosion potential compared to that in the absence of inhibitor. In literature, it has been also reported that if the displacement in E_{corr} is >85 mV the inhibitor can be seen as a cathodic or anodic type inhibitor and if the displacement of Ecorr is <85 mV, the inhibitor can be seen as mixed type [17]. In our study, the maximum displacement in E_{corr} value was 17 mV for MAN which indicates that the inhibitors acts as mixed type inhibitor.

2. Electrochemical impedance spectroscopy

The corrosion of mild steel in 1 M HCl solution in the presence of MAN was investigated by EIS at 308 K after an exposure period of 30 min. Nyquist plots for mild steel obtained at the interface in the absence and presence of MAN at different concentrations is given in Figure 3.

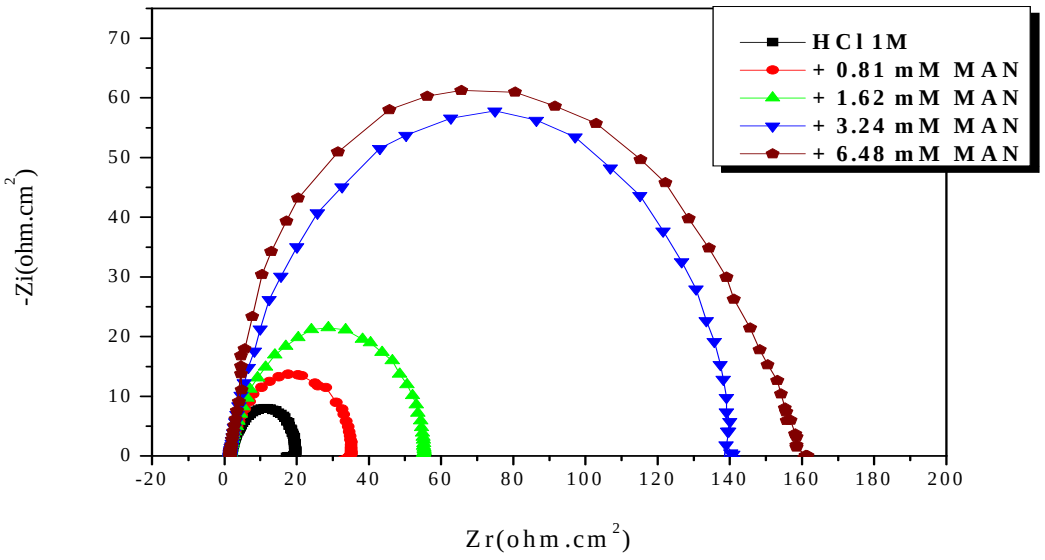

Figure 3. Nyquist plots for mild steel in 1 M HCl in the presence and absence of different concentrations of MAN.

As shown in Fig. 3, in uninhibited and inhibited 1 M HCl solutions, the impedance spectra exhibit one single capacitive loop, which indicates that the corrosion of steel is mainly controlled by the charge transfer process [18]. It is noted that these capacitive loops in 1 M HCl solutions are not perfect semicircles which can be attributed to the frequency dispersion effect as a result of the roughness and inhomogeneous of electrode surface [19]. Furthermore, the diameter of the capacitive loop in the presence of inhibitor is larger than that in blank solution, and enlarges with the inhibitor concentration. This indicates that the impedance of inhibited substrate increases with the inhibitor concentration, and leads to good inhibitive performance. The electrochemical parameters of R_t, C_{dl} and f_{max} derived from Nyquist plots and inhibition efficiency E_{Rt} (%) are calculated and listed in Table 2.

Table 2: Characteristic parameters evaluated from the impedance diagram for steel in 1 M HCl at various concentrations of MAN.

concentration (mM)	$R_s(\Omega.cm^2)$	$R_t(\Omega.cm^2)$	f_{max} (Hz)	C_{dl} (µF cm²)	E_{Rt} (%)
HCl 1 M	2.15	16.96	111.61	84.12	
0.81	2.37	32.42	50	98.23	47
1.62	1.85	53.24	40	74.77	68
3.24	2.13	137.3	25	46.39	87
6.48	1.31	158.8	20	50.13	89

From the impedance data in Table 2, we conclude that the R_t values increase with inhibitor concentration and consequently the inhibition efficiency (E_{Rt}) increases to 89 % at 6.48 mM. In fact, the presence of MAN is accompanied by the increase of the value of R_t in acidic solution confirming a charge transfer process mainly controlling the corrosion of mild steel. Values of double layer capacitance are also brought down to the maximum extent in the presence of inhibitor and the decrease in the values of C_{dl} follows the order similar to that obtained for I_{corr} in this study. The decrease in C_{dl} is due to the adsorption of the MAN on the metal surface leading to the formation of film or complex from acidic solution. We also note the increase of the value of R_t with the inhibitor concentration leading to an increase in the corrosion inhibition efficiency.

Moreover, the EIS results of these capacitive loops are simulated by the equivalent circuit shown in Figure 4 to pure electric models that could verify or rule out mechanistic models and enable the calculation of numerical values corresponding to the physical and/or chemical properties of the electrochemical system under investigation [20]. In the electrical equivalent circuit, R_s is the electrolyte resistance, R_t the charge transfer resistance and C_{dl} is the double layer capacitance.

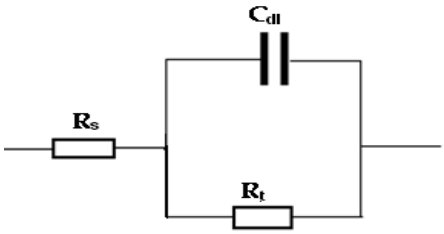

Figure 4. Equivalent circuit used to fit the EIS data of mild steel in 1 M HCl at different concentrations of MAN.

3. Weight loss measurement

The effect of addition of different concentrations of MAN tested at different temperatures on the corrosion of mild steel in 1 M HCl solution was studied by weight loss measurements after 6 h of immersion period. The values of percentage inhibition efficiency Ew (%) and corrosion rate (W) obtained are summarized in Table 3.

Table 3. Corrosion Parameters for mild Steel in 1 M HCl in absence and presence of different concentrations of MAN obtained from Weight Loss Measurements at different temperatures.

C (mM)	298		308		318		328	
	W (mg/cm^2.h)	E_w (%)	W (mg/cm^2.h)	E_w (%)	W (mg/cm^2.h)	E_w (%)	W (mg/cm^2.h)	E_w (%)
0	1.032		1.803		3.483		5.883	
0.81	0.362	64.92	0.744	58.75	1.556	55.32	3.229	45.12
1.62	0.276	73.25	0.553	69.34	1.329	61.85	2.861	51.37
3.24	0.143	86.13	0.462	74.35	1.063	69.47	2.416	58.94
6.48	0.102	90.12	0.264	85.34	0.727	79.14	1.986	66.24

3.1. Effect of MAN on corrosion rate (W)

The corrosion rate (W) obtained of mild steel in the absence and in the presence of various concentrations of MAN at different temperatures in 1 M HCl solutions after 6 h of immersion are shown in Figure 5.

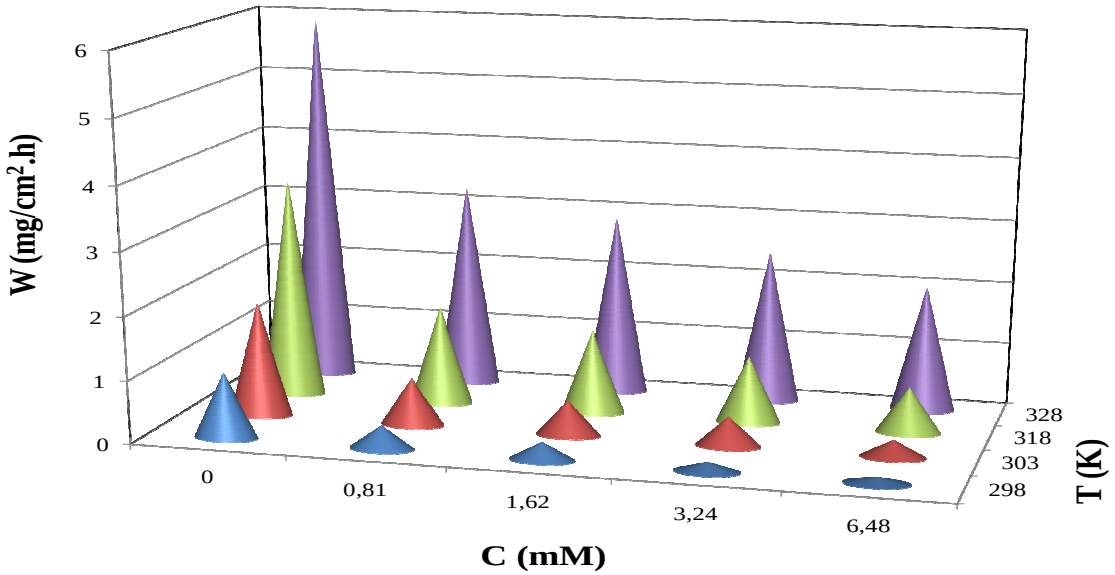

Figure 5. Variation of corrosion rate (W) as a function of temperature and concentration of MAN.

The results indicated that the corrosion rate (W) of mild steel decreased continuously with increasing the inhibitor concentration, ie, the corrosion of steel is retarded by MAN, or the inhibition enhances with the inhibitor concentration. This behavior is due to the fact that the adsorption coverage of inhibitor on steel surface increases with the inhibitor concentration. Also, the corrosion rate (W) increases with temperature both in uninhibited and

inhibited solutions, especially goes up more rapidly in the absence of inhibitor. These results confirm that MAN acts as an effective inhibitor in the range of temperature studied.

3.2. Effect of MAN on inhibition efficiency (E_w)

The values of E_w for different MAN concentrations at 298-328 K in 1 M HCl solution are presented in Figure 6.

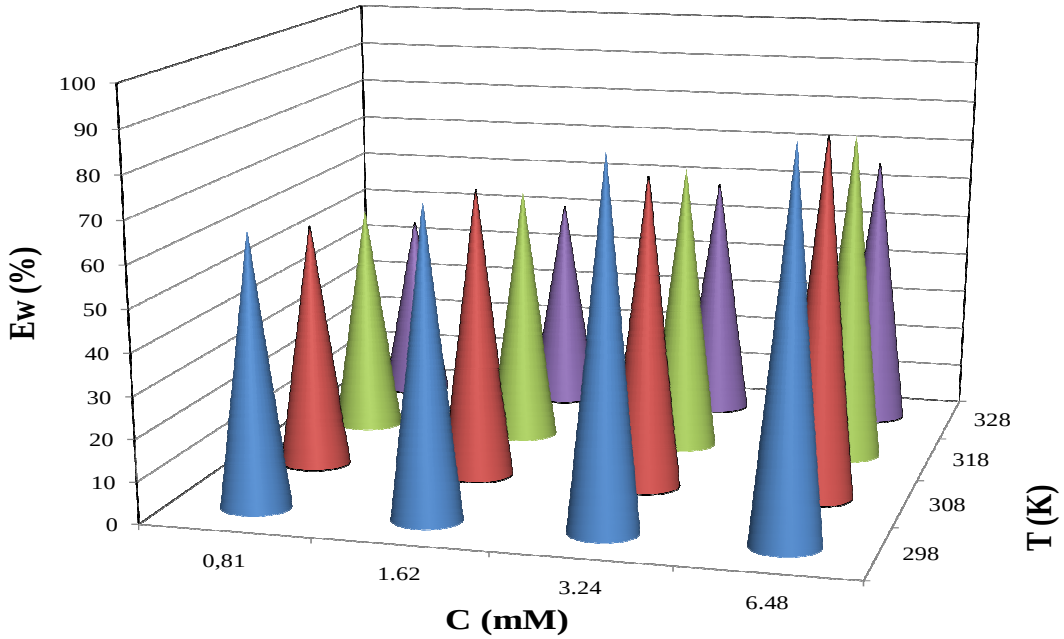

Figure 6. Relationship between inhibition efficiency (E_w) and temperature and concentration of MAN in 1 M HCl.

The results reveal that inhibition efficiency E_w increases sharply with increase in concentration of MAN, indicating that the extent of inhibition is dependent on the amount of MAN (concentration-dependent). Also, we note that the efficiency (E_w) depends on the temperature and increases with the rise of temperature from 298 to 343 K, and when the concentration reached to 6.48 mM, E_w of MAN reached a high values of 90.12 % in 1 M HCl solution at 298 K, which represents excellent inhibitive ability of MAN. The decrease in inhibition efficiency with increase in temperature may be attributed to the increased desorption of inhibitor molecules from metal surface and the increase in the solubility of the protective film or the reaction products precipitated on the surface of the metal that might otherwise inhibit the reaction.

The variation of inhibition efficiency (E %), determined by the three methods (weight loss, polarization curves and EIS methods), as a function of concentration of MAN in 1 M HCl show a good agreement with the three methods used in this investigation.

4. Kinetic and Activation parameters.

In order to calculate activation parameters of the corrosion reaction such as activation energy E°a, activated entropy ΔS°a and activation enthalpy ΔH°a for the corrosion of mild steel in acid solution in absence and presence of different concentrations of MAN, the Arrhenius equation (7) and its alternative formulation called transition state equation (8) were employed [21].

$$W = A\exp\left(-\frac{E^{\circ}_a}{RT}\right) \quad (7)$$

$$W = \frac{RT}{Nh}\exp\left(\frac{\Delta S^{\circ}_a}{R}\right)\exp\left(-\frac{\Delta H^{\circ}_a}{RT}\right) \quad (8)$$

where E°a is the apparent activation corrosion energy, T is the absolute temperature, R is the universal gas constant, A is the Arrhenius pre-exponential factor, h is he Plank's constant, N is the Avogrado's number, ΔS°a is the entropy of activation and ΔH°a is the enthalpy of activation.

Plotting the logarithm of the corrosion rate (W) versus reciprocal of absolute temperature, the activation energy can be calculated from the slope (-E°a/R). Figure 7 shows the variations of Ln (W) with the presence and absence of inhibitor with the (1/T).

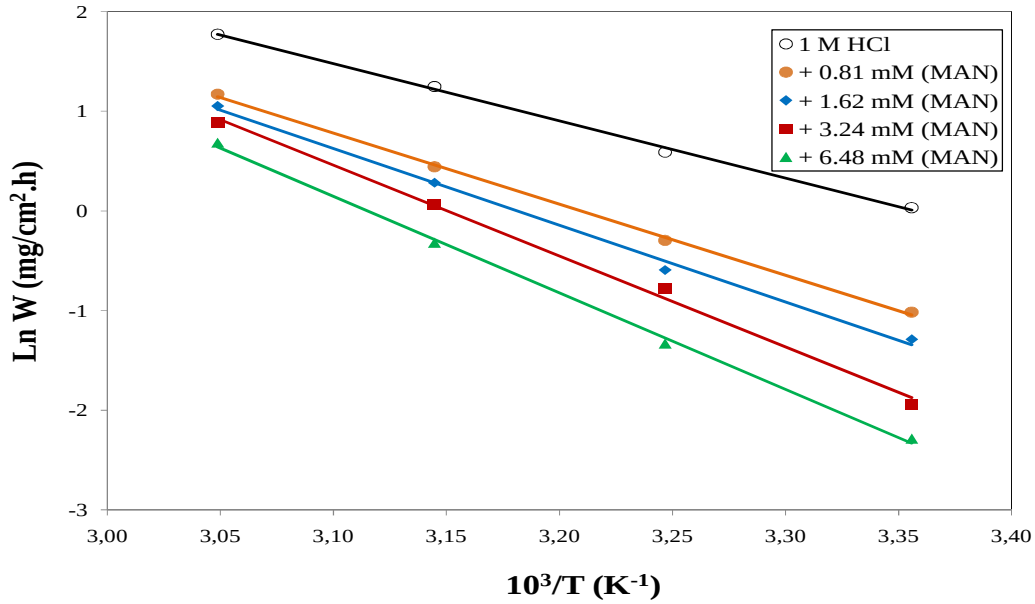

Figure 7. Arrhenius plots for mild steel corrosion rates (W) in 1 M HCl at different concentrations of MAN.

The logarithm of the corrosion rate of steel Ln (W) can be represented as straight-lines function of (10^3/T) with the linear regression coefficient (R^2) was close to 1, indicating that the corrosion of steel in hydrochloric acid without and with inhibitor follows the Arrhenius equation. The activation energy (E°a) values were calculated from the Arrhenius plots (Figure 7) and the results are shown in Table 4.

Further, using Eq. (8), plots of Ln (W/T) versus 10^3/T gave straight lines (Figure 8) with a slope of (-ΔH°a/R) and an intercept of (Ln(R/Nh) + (ΔS°a/R)) from which the values of ΔH°a and ΔS°a were calculated and are listed in Table 4.

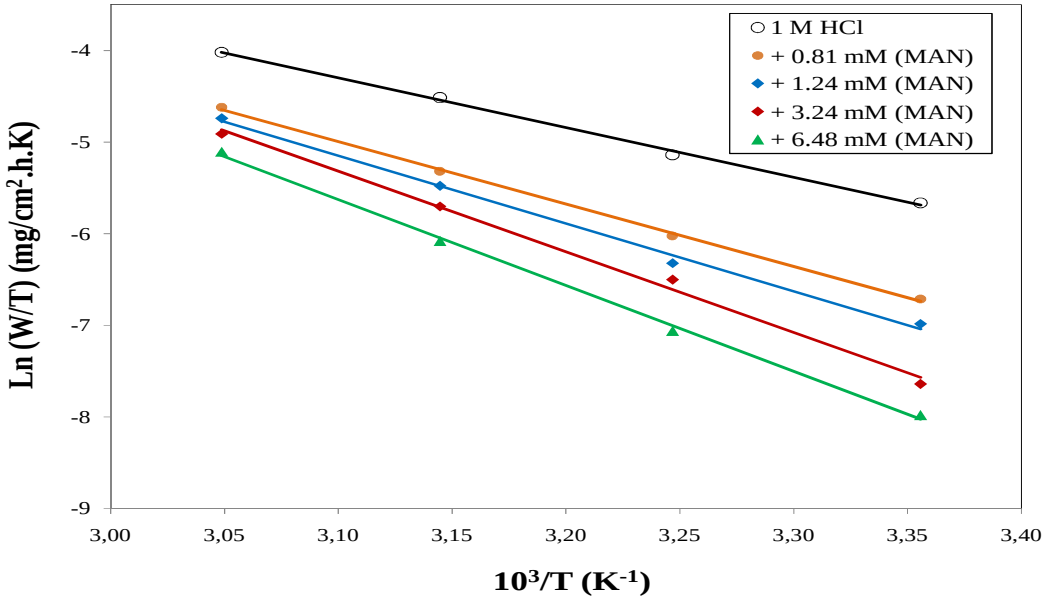

Figure 8. Transition-state plot for mild steel corrosion rates (W) in 1 M HCl in absence and presence of different concentrations of MAN.

The activation energies in the presence of MAN were observed higher than those in uninhibited acid solution (Table 4). This explains that the energy barrier of corrosion reaction increases with the concentration of MAN. It is clear from equation (7) that corrosion rate is influenced by $E°_a$. Generally, higher E°a value leads to the lower corrosion rate. In addition, the value of activation energy that is around 40–80 KJ.mol^{-1} can be suggested to obey the physical adsorption (physiosorption) mechanism [22]. Physiosorption is often related with this phenomenon, where an adsorptive film of electrostatic character is formed on the mild steel surface.

Table 4. Activation parameters E°a, ΔS°a, ΔH°a of the dissolution of steel in 1 M HCl at different concentrations of MAN.

C (mM)	E°a (KJ. mol^{-1})	ΔH°a (KJ.mol^{-1})	ΔS°a (J. mol-1.K^{-1})
0	47.78	45.19	- 93.35
0.81	59.33	56.74	- 63.40
1.62	64.11	61.50	- 44.92
3.24	75.87	73.28	- 14.81
6.48	80.59	77.80	- 0.25

The positive value of enthalpy of activation (ΔH°a) in the absence and presence of various concentration of inhibitor reflects the endothermic nature of mild steel dissolution process meaning that dissolution of steel is difficult [23]. It is evident from the table that the value of ΔH°a increased in the presence of MAN than the uninhibited solution indicating higher protection efficiency. This may be attributed to the presence of energy barrier for the reaction; hence the process of adsorption of inhibitor leads to rise in enthalpy of the corrosion process. The negative values of entropies of activation (ΔS°a) imply that the activated complex in the rate determining step represents an association rather than a dissociation step, meaning that a decrease in disordering takes place on going from reactants to the activated complex [24].

5. Adsorption considerations

Two main types of interaction can describe the adsorption of organic compounds namely: physical adsorption and chemical adsorption. These are dependent on the electronic structure of the metal, the nature of the electrolyte and the chemical structure of the inhibitor.

The character of adsorption of inhibitor in combination with halides was elucidated from the degree of surface coverage (θ) values calculated from the weight loss data ($\theta = E_w/100$) at different temperatures. The values of surface coverage, θ for the inhibitor have been used to explain the best isotherm to determine the adsorption process. Attempts were made to fit θ values to various adsorption isotherms namely Frumkin, Temkin. Langmuir and Freundlich.

It was assumed that the adsorption of MAN would follow the Langmuir adsorption isotherm. The plot of C/θ versus C (Fig. 9) yields a straight line with all linear correlation coefficients (R^2) are almost equal to 1, and the slope values are also close to 1, supporting the assumption that the adsorption of MAN from hydrochloric acid solution on the mild steel surface obeys a Langmuir adsorption isotherm, which is represented by Eq. (9).

$$\frac{C}{\theta} = \frac{1}{K} + C \qquad (9)$$

As shown in Table 5, the adsorptive equilibrium constant (K) decreases with the temperature in 1 M HCl solution, which could be ascribed to that it is easy for inhibitor to adsorb on the steel surface at relatively lower temperature. But when the temperature is gone up, the adsorbed inhibitor tends to desorb from the steel surface. Generally, large value of K is bound up with better inhibition efficiency of a given inhibitor. This is in good agreement with the values of E_w obtained from Fig. 6.

Thermodynamic parameters are important to further understand the adsorption process of inhibitor on steel/solution interface. The equilibrium adsorption constant, K is related to the standard Gibb's free energy of adsorption ($\Delta G°_{ads}$) with the following equation:

$$K = \frac{1}{55.5}.\exp\left(-\frac{\Delta G°_{ads}}{RT}\right) \qquad (10)$$

The standard adsorption enthalpy ($\Delta H°_{ads}$) could be calculated on the basis of Van't Hoff equation [25]:

$$LnK = -\frac{\Delta H°_{ads}}{RT} + D \qquad (11)$$

where R is the universal gas constant, T is the thermodynamic temperature, D is integration constant, and the value of 55.5 is the concentration of water in the solution in M (mol/L).

The standard adsorption enthalpy ($\Delta H°_{ads}$) can also be calculated from the Gibbs-Helmholtz equation:

$$\frac{\Delta G°_{ads}}{T} = \frac{\Delta H°_{ads}}{T} + k \qquad (12)$$

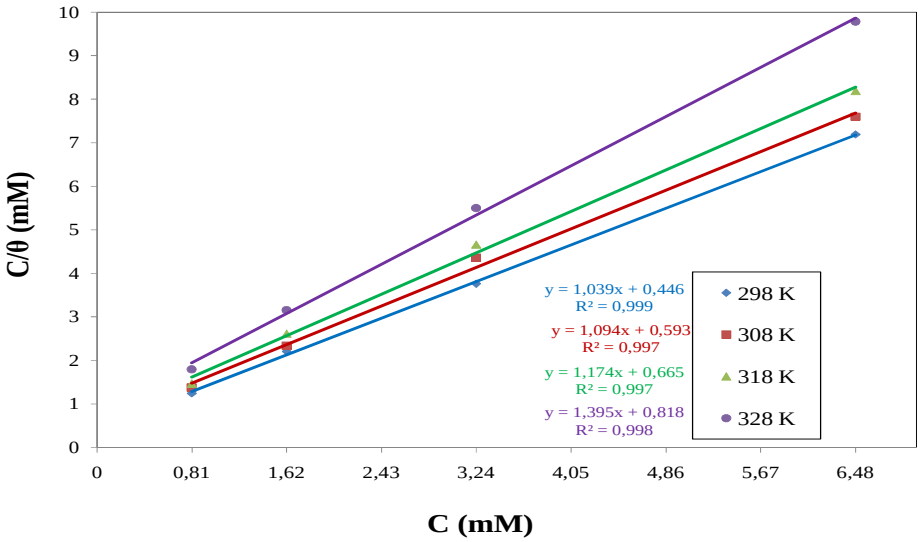

Figure 9. Langmuir adsorption isotherm of MAN on the mild steel surface in 1 M HCl at different temperatures.

To calculate the enthalpy of adsorption ($\Delta H°_{ads}$), LnK was plotted against 1/T (Figure 10) and straight line was obtained with slope equal to ($-\Delta H°_{ads}/R$). Also, the variation of $\Delta G°_{ads}/T$ vs 1/T gives straight line with slope equal to $\Delta H°_{ads}$ (Figure 11). With the obtained both parameters of $\Delta G°_{ads}$ and $\Delta H°_{ads}$, the standard adsorption entropy ($\Delta S°_{ads}$) can be calculated using the following thermodynamic basic Equ. (13). All the standard thermodynamic parameters are listed in Table 5.

$$\Delta S°_{ads} = \frac{\Delta H°_{ads} - \Delta G°_{ads}}{T} \qquad (13)$$

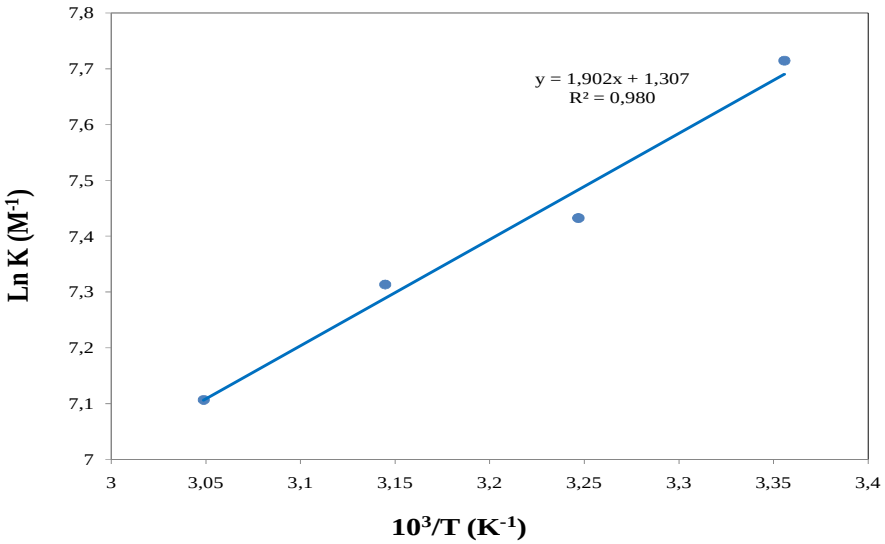

Figure 10. Van't Hoff's plot of Ln K against 1/T for the adsorption of MAN onto mild steel.

Table 5. Thermodynamic parameters for adsorption of MAN on mild steel in 1 M HCl solution at different temperatures from Langmuir adsorption isotherm.

Temperature (K)	R^2	K ($L.mol^{-1}$)	$\Delta G°_{ads}$ ($KJ.mol^{-1}$)	$\Delta H°_{ads}$ ($KJ.mol^{-1}$)	$\Delta S°_{ads}$ ($J.mol^{-1}.K^{-1}$)
298	0.999	2.24×10^3	- 29.08		44.50
308	0.997	1.69×10^3	- 29.33	- 15.82 Eq (11)	43.86
318	0.997	1.50×10^3	- 29.97	- 15.81 Eq (12)	44.50
328	0.998	1.22×10^3	- 30.35		44.30

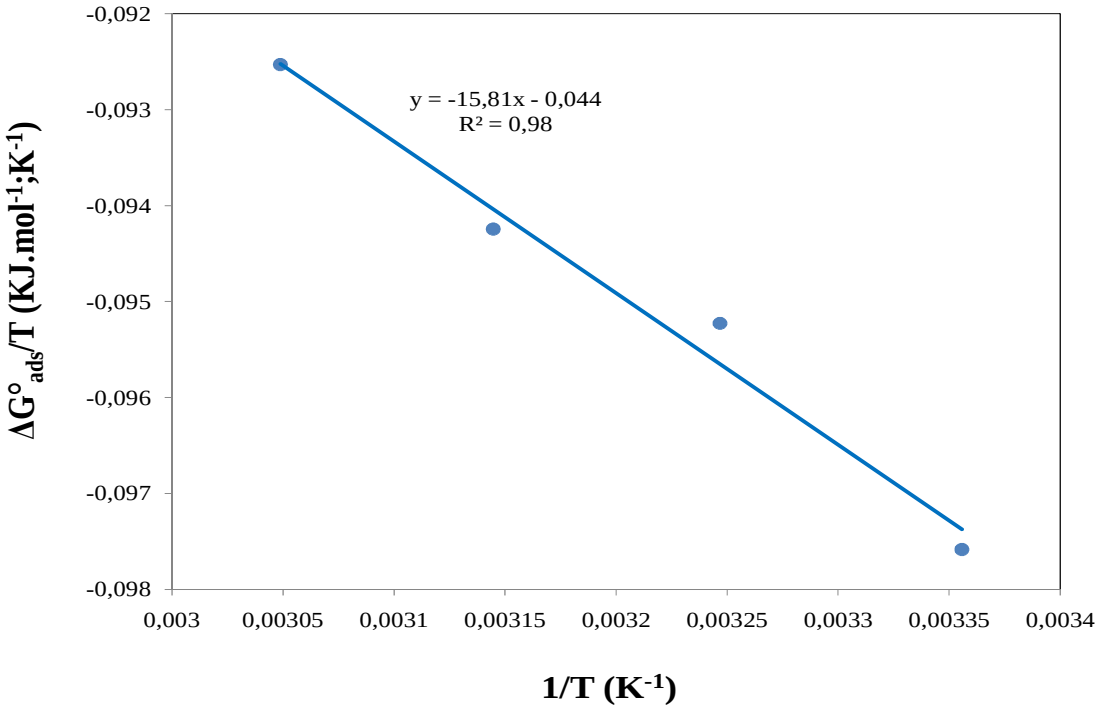

Figure 11. The relationship between ($\Delta G°_{ads}/T$) and 1/T.

The negative values of $\Delta G°_{ads}$ suggest (Table 5) that the adsorption of inhibitor molecules onto steel surface is a spontaneous phenomenon. It is well known that values of $\Delta G°_{ads}$ around −20 KJ.mol^{-1} or lower are associated with the physiosorption phenomenon where the electrostatic interaction assemble between the charged molecule and the charged metal, while those around −40 KJ.mol^{-1} or higher are associated with the chemiosorption phenomenon where the sharing or transfer of organic molecules charge with the metal surface occurs [26]. Here, the calculated ΔG^{0}_{ads} values are ranging between -29.09 and -30.35 kJ mol^{-1}, indicating that the adsorption mechanism of MAN on mild steel in 1 M HCl solution at the studied temperatures may be a combination of both electrostatic-adsorption and chemisorptions (comprehensive adsorption). However, physisorption was the major contributor, while chemisorption only slightly contributed to the adsorption mechanism judging from the decrease of IE% with increase in temperature [27].

In the present study, the value of $\Delta G°_{ads}$ computed and shown in Table 5 supports the physisorption of MAN on mild steel.

Also, the negative values of $\Delta H°_{ads}$ mean that the dissolution process is an exothermic phenomenon. The exothermic process is attributed to either physical or chemical adsorption or mixture of both whereas endothermic process corresponds to chemisorptions [28]. In an exothermic process, physisorption is distinguished from chemisorption by considering the absolute value of $\Delta H°_{ads}$. For physisorption process, the value of $\Delta H°_{ads}$ is lower than 40 Kj.mol^{-1} while the heat of adsorption for chemisorption process is approaches to 100 KJ.mol^{-1} [27]. In our study, the heat of adsorption is -15.82 KJ.mol^{-1} postulates that a physisorption is more favoured. The value of the enthalpy of adsorption found by the two methods such as Van't Hoff and Gibbs–Helmholtz relations (Eq (11) and Eq (12), respectively) are in good agreement.

Moreover, the positive value of $\Delta S°_{ads}$ in the presence of MAN is an indication of increase in solvent entropy. It also interpreted with increase of disorders due to more water molecules which can be desorbed from the metal surface by one inhibitor molecule. Therefore, it is revealed that decrease in the enthalpy is the driving force for the adsorption of the inhibitor on the surface of the metal [29].

6. Quantum chemical studies

DFT is considered as a very useful technique to probe the inhibitor/surface interaction as well as to analyze the experimental data. Figs. 12–15 show the optimized geometry, the HOMO density distribution, the LUMO density distribution and the Mulliken charge population analysis plots for MAN molecule obtained with DFT at B3LYP/6-31G (d) level of theory.

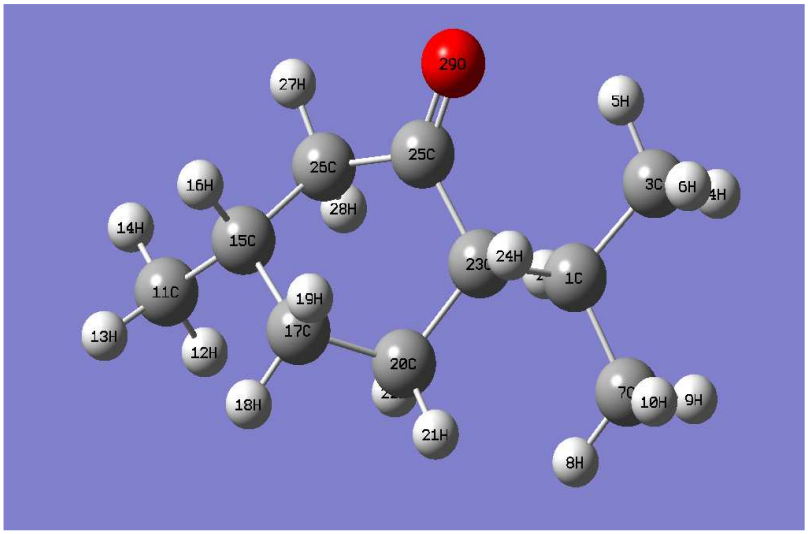

Figure 12. Optimized structure of menthone (MAN).

From Figs. 13 and 14, it could be seen that MAN might have can have different HOMO and LUMO distributions. The HOMO densities were mainly located on the entire menthone moiety and strongly distributed in the carbonyl group region, while the LUMO densities were concentrated on in the carbonyl group region. This kind of structure is difficult to form chemical bond active centers, which proved the probability of physical adsorption between the interaction sites [30]. Moreover, unoccupied d orbitals of Fe atom can accept electrons from the inhibitor molecule to form a coordinate bond while the inhibitor molecule can accept electrons from Fe atom with its anti-bonding orbitals to form back-donating bond.

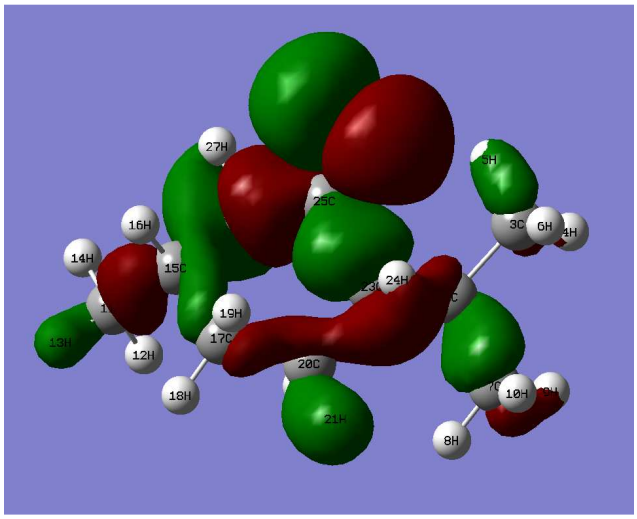

Figure 13. The highest occupied molecular orbital (HOMO) density (left) and the lowest unoccupied molecular orbital (LUMO) density (right) of MAN using DFT at the B3LYP/6-31G (d) basis set level.

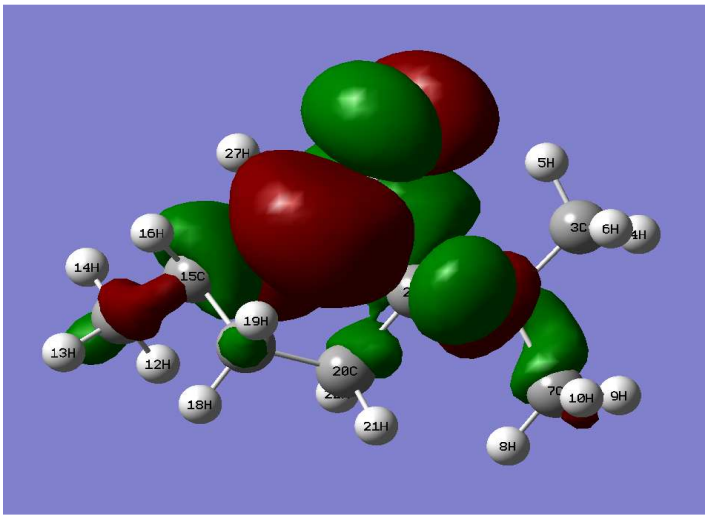

Figure 14. The highest occupied molecular orbital (HOMO) density (left) and the lowest unoccupied molecular orbital (LUMO) density (right) of MAN using DFT at the B3LYP/6-31G (d) basis set level.

The Mulliken charge of MAN is shown in Fig. 15. It is clear that the oxygen atom as well as some carbons atoms carries negative charge centers which could offer electrons to the mild steel surface to form a coordinate bond. Among them, the highest negative charge is domiciled in oxygen atom. This suggests that this active center with excess charges could act as a nucleophilic reagent. There is a general consensus by several authors that the more negatively charged heteroatom is, the more is its ability to adsorb on the metal surface through a donor–acceptor type reaction [31,32].

All other important quantum chemical parameters necessary for a meaningful discussion on the reactivity of MAN are reported in Table 6 namely the energy of the HOMO (E_{HOMO}), the energy of the LUMO (E_{LUMO}), the HOMO-LUMO energy difference (ΔE) and dipole moment (μ).

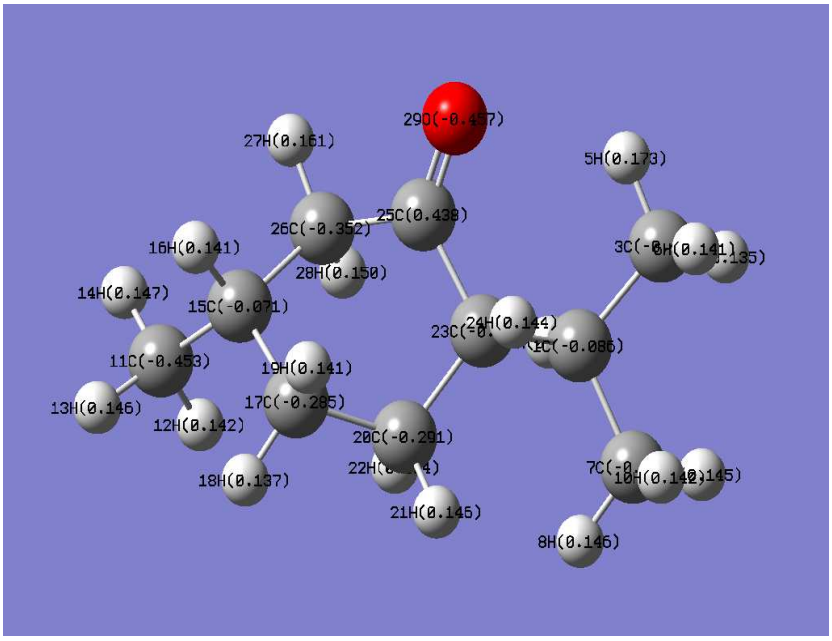

Figure 15. Mulliken charges population analysis of menthone (MAN) using DFT at the B3LYP/6-31G (d) basis set level.

Table 6. Some molecular properties of MAN calculated using DFT at the B3LYP/6-31G (d) basis set in aqueous phase.

Molecular parameters	**Calculated values**
Heat of formation (au)	- 467.138
Dipole moment (D)	2.90
E_{HOMO} (eV)	- 6.25 eV
E_{LUMO} (eV)	- 0.32 eV
ΔE (eV)	5.93 eV

It is well established in the literature that the higher the HOMO energy of the inhibitor, the greater the trend of offering electrons to unoccupied d orbital of the metal, and the higher the corrosion inhibition efficiency. In addition, the lower the LUMO energy, as the LUMO–HOMO energy gap decreased and the efficiency of inhibitor improved. Quantum chemical parameters listed in Table 6 reveal that MAN has high HOMO and low LUMO with high energy gap making it to exhibit a higher inhibitive effect obtained experimentally. Similar reports have been documented with comparable values obtained as the one reported in this work [33]. It has also been reported that increasing values of μ may facilitate adsorption (and therefore inhibition) by influencing the transport process through the adsorbed layer [34]. The dipole moment of MAN is 2.90 Debye (9.7 x 10^{-30} Cm), which is higher than that of H_2O (μ = 6.23 x 10^{-30} Cm). Accordingly, the adsorption of MAN molecules can be regarded as a quasi-substitution process between the MAN compound and water molecules at the electrode surface.

7. Explanation for inhibition

The adsorption process is affected by the chemical structure of inhibitor, the nature and charged surface of the metal and the distribution of charge over the whole inhibitor molecule. In general, owing to the complex nature of adsorption and inhibition of a given inhibitor, it is impossible for single adsorption mode between inhibitor molecules and metal surface. Molecule adsorption of the MAN at the metal surface should also be considered due to the interaction between the unshared electron pairs in the molecule and the metal.

In this study, the adsorption of the menthone on the metal surface is through the already adsorbed chloride ion. In acidic solutions, the menthone molecules exist as cations and adsorb through electrostatic interactions between the positively charged molecules and the metal surface negatively charged, due to adsorption of an excess of ions Cl^- in the first time. Owing to the acidity of the medium, the MAN can exist as a neutral species or in the cationic form. Thus, the adsorption of the neutral MAN molecules could occur due to the formation of links between the d orbital of iron atoms, involving the displacement of water molecules from the metal surface, and the lone sp^2 electron pairs present on the O atom [35].

Conclusion

Menthone (MAN) showed excellent inhibition performance for mild steel corrosion in 1 M HCl medium. The inhibition efficiencies, obtained from weight loss measurement, polarization and EIS techniques, increased with the concentration of MAN. From weight loss measurements, is clear that inhibition efficiency values decreased with increase temperature. The results of polarization curves revealed clearly that MAN showed excellent inhibition performance as a mixed-type inhibitor for mild steel corrosion in acidic solution. The results of EIS measurements indicated that the corrosion of steel is mainly controlled by the charge transfer process. Enthalpy of activation reflects the endothermic nature of the mild steel dissolution process. The adsorption behavior can be described by the Langmuir adsorption isotherm. Gibbs free energy of adsorption, enthalpy of adsorption and entropy of adsorption indicated that the adsorption process is spontaneous and exothermic and the molecules adsorbed on the metal surface by the process of physical adsorption. Data obtained from quantum chemical calculations using DFT at the B3LYP/6-31G (d) level of theory were correlated to the inhibitive effect of menthone.

References

1. Eghbali F., MoayedM.H., Davoodi A., Ebrahimi N., *Corros. Sci*. 53 (2011) 513.
2. Bentiss F., Lebrini M., Traisnel M,. Lagrenee M., *J. Appl. Electrochem*. 39 (2009) 1399.
3. Okafor P.C., Ikpi M.E., Uwaha I.E., Ebenso E.E., Ekpe U.J., Umoren S.A., *Corros. Sci*. 50 (2008) 2310.
4. Mihit M., Laarej K., Abou El Makarim H., Bazzi L., Salghi R., Hammouti B., *Arab. J. Chem*. 3 (2010) 55.
5. Zarrouk A., Hammouti B., Zarrok H., Salghi R., Bouachrine M., Bentiss F., Al-Deyab S.S., *Res. Chem. Intermed*. 38 (2012) 2327.
6. Barouni K., Bazzi L., Salghi R., Mihit M., Hammouti B., Albourine A., El Issami S., *Mater. Lett*. 62 (2008) 3325.
7. Abdel-Gaber AM., Abd-El-Nabey BA., Saadawy M ., *Corros. Sci*.51 (2009) 1038.
8. Raja P.B., Sethuraman. MG. *Mater. Lett*. 62 (2008) 113.
9. Bouyanzer A., Hammouti B., Majidi L., *Mater. Lett*. 60 (2006) 2840.
10. Faska Z., Belliou A., Boukla M., Majid L., Fih, R., Bouyanzer A., Hammouti B., *Monatsh. Chem*. 139 (2008) 1417.
11. Lahhit N., Bouyanzer A., Desjobert J.M., Hammouti B., Salghi R., Costa J., Jama C., Bentiss F., Majidi L., Portug. *Electrochem. Acta*. 29 (2011) 127.
12. Chaieb E., Bouyanzer A., Hammouti B., Berrabah M., *Acta Phys. Chim. Sin*. 25 (2009) 1254.
13. Arctander S., Perfume and Flavour Chemicals (Aroma chemicals) II., No. 2053. Montclair, New York (1969).
14. Tsuru T., Haruyama S., Gijutsu B., *J. Jpn. Soc. Corros. Eng*. 27 (1978) 573.
15. Khaled K.F., *Electrochim. Acta* 48 (2003) 2493.
16. Lashkari M., Arshadi M.R., *J. Chem. Phys*. 299 (2004) 131.
17. Satapathy A.K., Gunasekaran G., Sahoo, S.C., Amit, k., Rodrigues, P.V., *Corros. Sci*. 51 (2009) 2848.
18. Sathiyapriya A.R., Muralidharan V.S., Subramanian. *Corrosion*. 64 (2008) 541.
19. Mansfel F., Kendig M.W., Tsai S., *Corrosion*. 38 (1982) 570.
20. Benabdellah M., Aouniti A., Dafali A., Hammouti B., Benkaddour M., Yahyi A., Ettouhami A., A*ppl. Surf. Sci*. 252 (2006) 8341.
21. Bentiss F., Traisnel, M., Lagrenee. M., *Corros. Sci*. 42 (2000) 127.
22. Orubite K.O., Oforka, N.C., *Mater. Lett*. 58 (2004) 1768.
23. Guan N.M., Xueming, L., Fei, L., *Chem. Phys*. 86 (2004) 59.
24. Samkarapapaavinasam, S., Ahmed M.F., *J. Appl. Electrochem*. 22 (1992) 390.
25. Libin, T., Guannan, M., Guangheng, L., *Corros. Sci*. 45 (2003) 2251.
26. Khamis E., Bellucci F., Latanision R., El-Ashry E.S., *Corrosion*. 47 (1991) 677.
27. Noor E.A., Al-Moubaraki A.H.., *Mater. Chem. Phys*. 110 (2008) 145.
28. Bentiss F., Lebrini M., Lagrenée M., *Corros. Sci*. 47 (2005) 2915.
29. Gulsen A., *Coll. Surf*. 317 (2005) 730.
30. Yan Y., Li W., Cai L., Hou B., *Electrochim. Acta*, 53 (2008) 5953.
31. Gao G., Liang C., *Electrochim. Acta*, 52 (2007) 4554.
32. Obot I.B., Obi-Egbedi N.O., Odozi N.W., *Corros. Sci*. 52 (2010) 923.
33. Obot I.B., Obi-Egbedi N.O., *Corros. Sci*. 52 (2010) 198.
34. Wang H., Wang X., Wang H., Wang L., Liu, A., *Mol. J., Model*. 13 (2007) 147.
35. Herrag L., Hammouti B., Elkadiri S., Aouniti A., Jama C., Vezin H., Bentiss F., *Corros. Sci*. 52 (2010) 3042.